SCIENTIFIC REPORTS

OPEN

SUBJECT AREAS:
FERROMAGNETISM
COMPOSITES
ELECTRONIC DEVICES
MAGNETIC PROPERTIES AND MATERIALS

Received
22 March 2013

Accepted
10 July 2013

Published
26 July 2013

Correspondence and requests for materials should be addressed to Z.H.C. (zhcheng@iphy.ac.cn)

* Theses authors contributed equally to this work.

# Integrating giant microwave absorption with magnetic refrigeration in one multifunctional intermetallic compound of $LaFe_{11.6}Si_{1.4}C_{0.2}H_{1.7}$

Ning-Ning Song*, Ya-Jiao Ke*, Hai-Tao Yang, Hu Zhang, Xiang-Qun Zhang, Bao-Gen Shen & Zhao-Hua Cheng

State Key Laboratory of Magnetism and Beijing National Laboratory for Condensed Matter Physics, Institute of Physics, Chinese Academy of Sciences, Beijing 100190, China.

**Both microwave absorption and magnetocaloric effect (MCE) are two essential performances of magnetic materials. We observe that $LaFe_{11.6}Si_{1.4}C_{0.2}H_{1.7}$ intermetallic compound exhibits the advantages of both giant microwave absorption exceeding −42 dB and magnetic entropy change of −20 $Jkg^{-1}K^{-1}$. The excellent electromagnetic wave absorption results from the large magnetic loss and dielectric loss as well as the efficient complementarity between relative permittivity and permeability. The giant MCE effect in this material provides an ideal technique for cooling the MAMs to avoid temperature increase and infrared radiation during microwave absorption. Our finding suggests that we can integrate the giant microwave absorption with magnetic refrigeration in one multifunctional material. This integration not only advances our understanding of the correlation between microwave absorption and MCE, but also can open a new avenue to exploit microwave devices and electromagnetic stealth.**

The extensive development and use of the electronic devices have created a new kind of problem called electromagnetic interference (EMI). To suppress the serious EMI problem, it is becoming very urgent to design and fabricate the electromagnetic compatibility (EMC) devices, which can ensure that equipment items will not interfere with or prevent each other's correct operation through spurious emission. For achieving sufficient EMC, researchers have long been involved in exploiting microwave absorbing materials (MAMs) due to their prospective applications in electronic devices, military affairs such as airplanes, steamboats, tanks, microwave darkrooms, and even broadband electromagnetic cloaking[1,2]. Up to date, various MAMs composed of magnetic loss powders such as ferrite, nickel, cobalt, and dielectric loss materials such as carbon nanotubes (CNTs) and conducting polymers have been fabricated[3–8]. Two approaches, either making electromagnetic wave disappearance by interference(Figure 1(a)), or absorbing electromagnetic wave effectively and converting electromagnetic energy into heat, are generally adopted for microwave loss. Unfortunately, the temperature increment and infrared radiation of MAMs due to the conversion of electromagnetic energy into heat will seriously hamper the application of microwave devices and electromagnetic stealth(Figure 1(b)). Therefore, it is interesting to explore whether MAMs can be refrigerated during microwave absorption (Figure 1(c)).

Compared with traditional gas-compression/expansion refrigeration, magnetic refrigeration exhibits the advantages of high energy efficiency and environment friendliness[9–13]. The discovery of a giant magnetic entropy change in $La(Fe_{1-x}Si_x)_{13}$ intermetallic compounds gives rise to interest in searching for novel magnetic refrigerants[14,15]. Both microwave absorption and magnetocaloric effect (MCE) are two essential performances of magnetic materials. Meanwhile, to our knowledge, microwave properties of these novel magnetic refrigerants have never been reported. According to the Snoek limit[16], the product of the high frequency susceptibility, $\chi = \mu - 1$, and the resonance frequency, $f_r$, is proportional to the saturation magnetization, $(\mu - 1)f_r \propto M_S$, where $\mu$ is permeability. In addition, the upper limit of magnetic entropy change is determined by the relation of $\Delta S_M^{Max} = R\ln(2J+1)$, where $R$ is the gas constant and $J$ is the total angular momentum of the magnetic ion. The high saturation magnetization is thus one of prerequisites for achieving both high frequency permeability and giant magnetic entropy change. Among the rare-earth-Fe intermetallic compounds, $LaFe_{13-x}Si_x$ intermetallics have the most abundant Fe concentration, and consequently possesses high saturation magnetization.

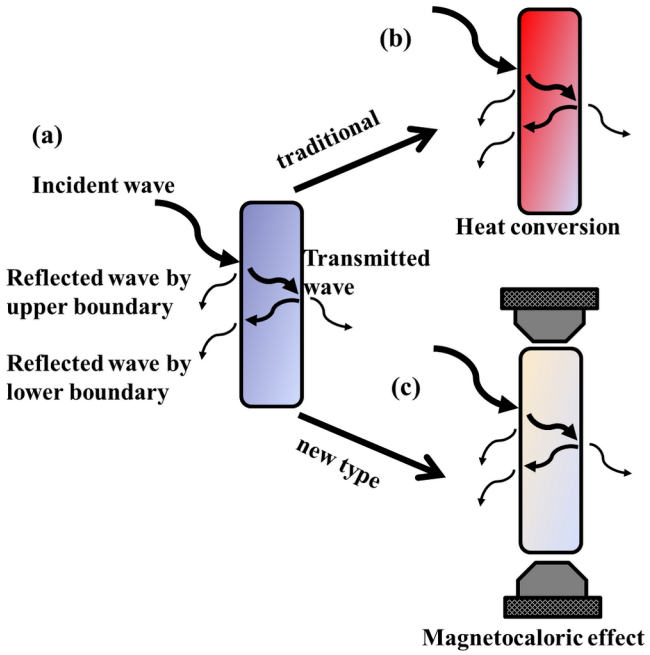


**Figure 1 | The scheme of microwave incident on an absorbing layer.** Two approaches, either making electromagnetic wave disappearance by interference (a), or absorbing electromagnetic wave effectively and converting electromagnetic energy into heat, are generally adopted for microwave loss (b). A prototype of magnetic cooling MAMs during microwave absorption (c) .

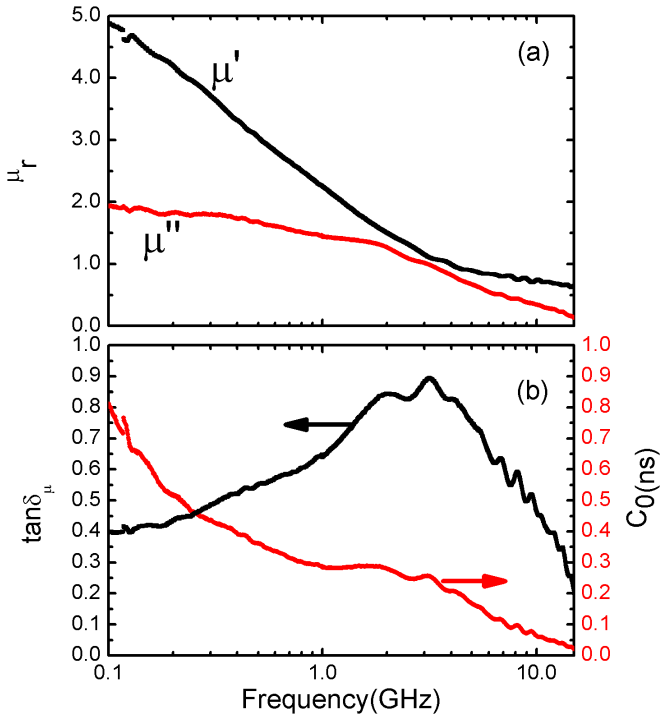


**Figure 2** | (a) Frequency dependence of relative complex permeability $\mu_r = \mu' - j\mu''$; and (b) magnetic loss tangent $\tan\delta_\mu = \mu''/\mu'$ of the $LaFe_{11.6}Si_{1.4}C_{0.2}H_{1.7}$/paraffin wax.

Here, we present the microwave absorption and magnetic entropy change of $LaFe_{11.6}Si_{1.4}C_{0.2}H_{1.7}$ intermetallic compound. $LaFe_{11.6}Si_{1.4}C_{0.2}H_{1.7}$ intermetallic compound shows a metallic behavior with resistivity value of 3.8 $\mu\Omega\bullet m$ at room temperature. The MAM must contain a sufficient quantity of free charge carriers in order to interact with microwave radiation. In order to reduce the eddy current loss induced by electromagnetic wave, the MAM sample was mixed metallic powders with insulating paraffin wax. To satisfy the microwave devices application above room temperature, the Curie temperature up to 330 K is achieved by the addition of interstitial atoms C and H. In the case of $LaFe_{11.6}Si_{1.4}C_{0.2}H_{1.7}$ intermetallic compound, Fe atoms occupy two sites, 8b and 96i, the Curie temperature is determined by the overall exchange interaction between Fe(8b)-Fe(8b), Fe(8b)-Fe(96i) and Fe(96i)-Fe(96i) atoms. Our previous neutron diffraction work demonstrated that the bond-length of Fe(8b)-Fe(96i) is very short, resulting a negative exchange interaction between Fe(8b) and Fe(96i), and consequently weakens the overall exchange interaction. The addition of interstitial atoms C and H leads to an expansion of the bond-length of Fe(8b)-Fe(96i) and a change in sign of Fe(8b)-Fe(96i) exchange interaction from negative to positive[17]. Therefore, the overall exchange interaction between Fe-Fe atoms and the Curie temperature are significantly enhanced by the introduction of interstitial atoms C and H. We observe that this intermetallic compound exhibits the advantages of both giant microwave absorption exceeding −42 dB and magnetic entropy change of $-20\ Jkg^{-1}K^{-1}$. The value of *RL* for $LaFe_{11.6}Si_{1.4}C_{0.2}H_{1.7}$/paraffin wax is comparable with that of the most common used microwave absorber, carbonyl iron (35 dB) and conventional ferrite MAMs (30 dB)[18,19]. Our finding suggests that we can integrate the microwave absorption with magnetic refrigeration in one multifunctional material. This integration not only gives us a deeper insight into the effect of intrinsic magnetic properties on the performances of microwave absorption and MCE, but also provides a new possibility for solving the bottleneck of microwave devices and electromagnetic stealth.

## Results

Figures 2(a) and 2(b) illustrates the frequency dependence of relative complex permeability $\mu_r = \mu' - j\mu''$ magnetic loss tangent $\tan\delta_\mu = \mu''/\mu'$ of the $LaFe_{11.6}Si_{1.4}C_{0.2}H_{1.7}$/paraffin wax, respectively. Both the real part ($\mu'$) and the imaginary part ($\mu''$) of relative complex permeability($\mu_r = \mu' - j\mu''$) for the sample of $LaFe_{11.6}Si_{1.4}C_{0.2}H_{1.7}$/paraffin wax exhibit a relaxation behavior and decreases from 4.9 to 1.0, and from 1.9 to 1.0 as frequency increase up to 3.2 GHz, respectively (Figure 2(a)). The magnetic loss tangent $\tan\delta_\mu = \mu''/\mu'$ increases first with frequency, reaches a broad peak value of 0.89 at 3.2 GHz, and decreases with further increasing frequency (Figure 2(b)). It is known that the microwave magnetic loss of magnetic materials originates mainly from hysteresis, domain wall resonance, eddy current effect and the natural ferromagnetic resonance. Since almost no hysteresis loops can be observed from the magnetization curves measured during increasing and decreasing magnetic field processes (as will mention latter), the hysteresis loss resulted from irreversible magnetization is negligible. In our study, the permeability was measured over a frequency range of 0.1–15.0 GHz, the contribution of domain wall resonance is neglected since it occurs usually in the 1–100 MHz range. The eddy current loss is related to the diameter of particles $d$ and the electric conductivity $\sigma$, which can be expressed by $\mu' \approx 2\pi\mu_0(\mu')^2\sigma d^2 f/3$, where $\mu_0$ is the permeability of vacuum. If the magnetic loss only results from eddy current loss, the value of $C_0$ ($C_0 = \mu''/(\mu')^2 f = 2\pi\mu_0\sigma d^2/3$) should be a constant with varying frequency[20]. The values of $C_0$ significantly decrease with increasing frequency from 0.1 to 15.0 GHz, suggesting the magnetic loss is not related to eddy current (Figure 2(b)). Therefore, the very broad peak of magnetic loss is mainly caused by the natural ferromagnetic resonance.

It is known that the real permittivity ($\varepsilon'$) is an expression of polarization ability of a material which mainly arises from dipolar polarization and interfacial polarization at microwave frequency[21]. The imaginary permittivity ($\varepsilon''$) follows the relation $\varepsilon' \approx 1/2\pi\varepsilon_0\rho f$ according to free-electron theory, where $\rho$ is the resistivity[22]. Both the real

part $\varepsilon'$ and the imaginary part $\varepsilon''$ of relative complex permittivity ($\varepsilon_r = \varepsilon' - j\varepsilon''$) for the sample of $LaFe_{11.6}Si_{1.4}C_{0.2}H_{1.7}$/paraffin wax are expected to decrease with increasing frequency (Figure 3(a)). The dielectric loss tangent $\tan\delta_\varepsilon$ keeps almost constant of 0.35 in the frequency range of 0.1–5.0 GHz, and reaches a maximum value of 0.46 around 8.2 GHz (Figure 3(b)). For comparison, the data of paraffin wax were also plotted in Figures 3(a) and 3(b). The dielectric loss for paraffin wax is about at least one order of magnitude smaller and can be ignored. Although the fundamental understanding of what determines the dielectric loss tangent has still not been established[8], we can concluded the displacement current by free carriers in $LaFe_{11.6}Si_{1.4}C_{0.2}H_\delta$ is main source of dielectric loss in this composite compound. The large values of the dielectric loss owing to highly conductive $LaFe_{11.6}Si_{1.4}C_{0.2}H_\delta$ are favorable for improving the microwave absorption properties. By comparing the frequency-dependence of dielectric loss with magnetic loss, the peak of $\tan\delta_\varepsilon$ occurs usually in higher frequency range.

To further confirm the magnetic loss and dielectric loss, the reflected loss (*RL*) of the sample was investigated. According to the transmission line theory, for a single layer absorber with a backed metal plate, the *RL* were simulated from the electromagnetic parameters at various sample thicknesses by means of the following expressions[23,24].

$$Z_{in} = Z_0(\mu_r/\varepsilon_r)^{1/2}\tanh[j2\pi fd/c](\mu_r\varepsilon_r)^{1/2} \quad (1)$$

$$RL = 20\log|(Z_{in} - Z_0)/(Z_{in} + Z_0)| \quad (2)$$

where $f$ is the frequency of the electromagnetic wave, $d$ is the thickness of the sample, $c$ is the velocity of light, $Z_0$ is the impedance of air, and $Z_{in}$ is the input impedance of the sample.

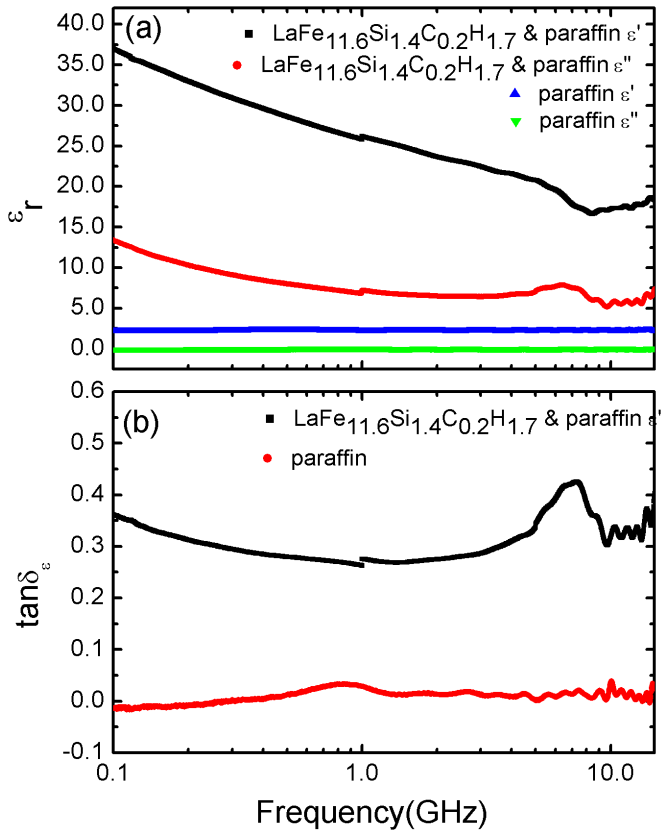


**Figure 3** | (a) Frequency dependence of relative complex permittivity $\varepsilon_r = \varepsilon' - j\varepsilon''$, and (B) dielectric loss tan $\delta_\varepsilon = \varepsilon''/\varepsilon'$ of the $LaFe_{11.6}Si_{1.4}C_{0.2}H_{1.7}$/paraffin wax. For comparison, the data of paraffin were also plotted.

The *RL* curves are governed by the contribution of electromagnetic wave interference from interface and by the microwave absorption. Considering the incident electromagnetic wave reflected by both the upper and lower boundaries of a thin film, the path difference of the reflected waves must be calculated in order to determine the condition for interference (figure 1(a)). According to the quarter-wave length matching model, the reflected wave and the incident wave will be out of phase by 180° at a certain frequency point, and cancel each other for the thickness of the sample satisfying the quarter-wavelength thickness relation[25].

$$t_m = \frac{n}{4}\lambda_m = \frac{nc}{4f_m\sqrt{|\varepsilon_r\mu_r|}}(n = 1,3,5\ldots) \quad (3)$$

where $f_m$ is the peak frequency of *RL*, $t_m$ is the thickness of the sample.

When the sample thickness satisfies the quarter or three-quarter of wave-length criteria, a peak or two peaks of *RL* appear (Figure 4). The optimal reflectivity loss of $RL = -42.5$ dB is reached at 2.7 GHz for 7.00 mm thickness. Since the *RL* is mainly deterined by the incident electromagnetic wave reflected by both the upper and lower boundaries of a thin film, its peak is sharper than theat of magnetic loss as shown in Figure 2(c).

In addition, as shown in the projection of *RL* in the basal plane, the peaks of *RL* obviously shift to lower frequencies with increasing the sample thickness. The *RL* value of −20 dB is comparable to the 99% of electromagnetic wave absorption according to Eqs. (1) and (2), and thus "$RL < -20$ dB" is considered as an adequate electromagnetic absorption at a microwave frequency. For our samples, the $RL < -20$ dB can be obtained in the 2.0–12.0 GHz range for the absorber thickness of 2.5–8.3 mm. Moreover, owing to the large magnetic loss tangent and dielectric loss tangent, a considerably large $RL = -10$ dB can be obtained in whole frequency range of 0.1–15 GHz and thickness of 1.0–8.3 mm, suggesting that this compound is an excellent candidate for MAMs. An effective MAMs need to satisfy the impedance matching condition, $\mu_r/\varepsilon_r \approx 1$.

The large magnetic loss and dielectric loss are favorable for excellent broadband EMC application. Unfortunately, the conversion of electromagnetic energy into heat will increase the MAMs temperature, which restricts the miniaturization and rapid increase in frequencies of electric devices. Moreover, the increase in MAMs temperature leads to infrared radiation since infrared light includes most of the thermal radiation emitted by objects near room temperature. The infrared radiation of MAMs will seriously hamper their application for electromagnetic stealth. Magnetic refrigeration based on MCE is a promising technique for cooling the MAMs during microwave absorption. To understand the MCE, we measured the isothermal magnetization curves of $LaFe_{11.6}Si_{1.4}C_{0.2}H_{1.7}$ in the temperature range of 300–350 K with an interval of 2 K. Owing to the low anisotropy field, the magnetization curve at room temperature

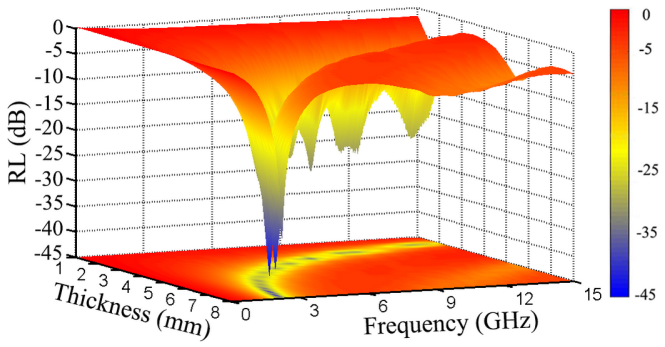


**Figure 4** | **Frequency- and thickness- dependence of refection loss (*RL*) for the $LaFe_{11.6}Si_{1.4}C_{0.2}H_{1.7}$/paraffin wax samples with different thickness.**

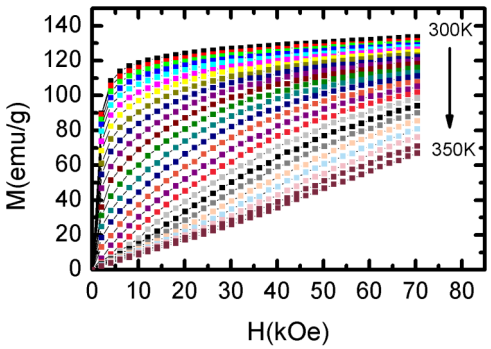


**Figure 5 | Isothermal magnetization curves of $LaFe_{11.6}Si_{1.4}C_{0.2}H_{1.7}$ in the temperature range of 300–350 K with an interval of 2 K.**

increases sharply with applied field (Figure 5). Moreover, we also observed that almost no hysteresis loops can be discerned from the magnetization curves measured either during heating and cooling processes or during increasing and decreasing magnetic field processes. No hysteresis loops is advantageous for the application of magnetic refrigeration[10].

At temperature $T$, the magnetic entropy change due to applied field $H$ can be calculated from the isothermal curves by the Maxwell relation

$$\Delta S_M(T,H) = \int_0^H \left(\frac{\partial M}{\partial T}\right)_H dH \qquad (4)$$

Figure 6 displays magnetic entropy change $\Delta S_M$ as a function of $T$ and $H$ of $LaFe_{11.6}Si_{1.4}C_{0.2}H_{1.7}$. From the calculated $\Delta S_M$ as a fuction of $T$ and $H$, a giant magnetic entropy change of $-20$ $Jkg^{-1}K^{-1}$ can be achieved at temperature around 330 K and applied field of 70 kOe. It is noteworthy that the MCE is not only governed by the magnetic entropy change, but also the refrigeration capacity (*RC*). The *RC* can be calculated by integrating the area under $-\Delta S_M$ *vs* $T$ curves within the temperature range at half-maximum of the peak. The *RC* was observed to increase with applied field (Figure 7).

## Discussion

In order to demonstrate the useful cooling power above room temperature, Zimm et al. constructed a rotary magnetic refrigerator through a 15 kOe $Nd_2Fe_{14}B$ permanent magnet. They found that the peak cooling capacity of LaFeSiH compares favorably with that of Gd[26]. Although the value of $-\Delta S_M = 7.5$ $Jkg^{-1}K^{-1}$ at 20 kOe is smaller than that of $La(Fe_{1-x}Si_x)H_y$ reported by Fujita et al.[27], the

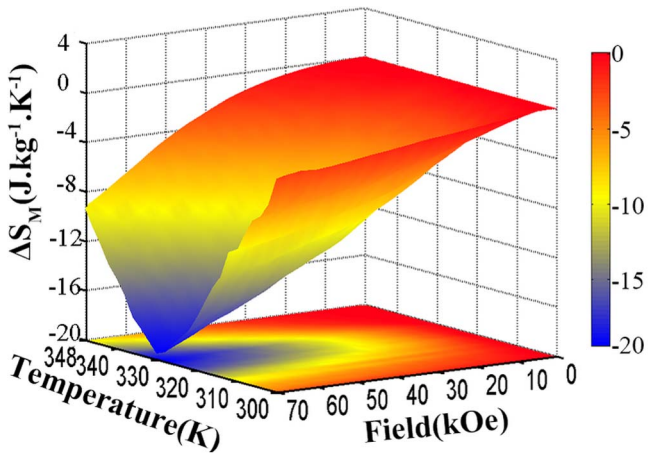


**Figure 6 | Magnetic entropy change $\Delta S_M$ as a function of $T$ and $H$ of $LaFe_{11.6}Si_{1.4}C_{0.2}H_{1.7}$.**

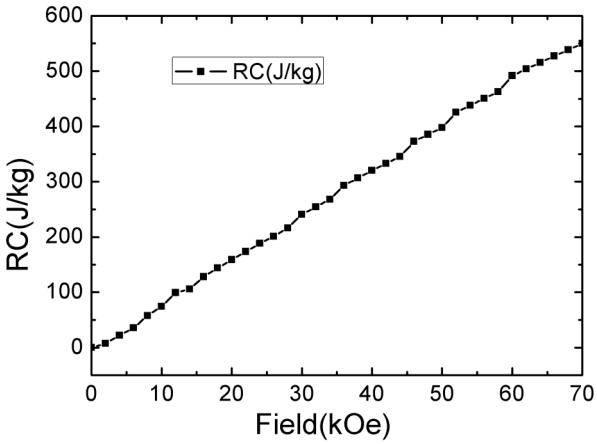


**Figure 7 | Field-dependence of refrigeration capability *RC* of $LaFe_{11.6}Si_{1.4}C_{0.2}H_{1.7}$.**

value of $RC = 158$ J/kg owing the broad peak of magnetic entropy change of our sample suggests that $LaFe_{11.6}Si_{1.4}C_{0.2}H_{1.7}$ compound is also a promising magnetic refrigerant.

One may further concern whether the reflection loss is reduced by the applied field during magnetic refrigeration process. Figure 8 illustrates the reflection loss for the sample with thickness of 2.0 mm measured in the applied field ranging from 0 to 1900 Oe. Since the applied magnetic field may decrease magnetic permeability at low frequency range, the reflection loss is slightly reduced with increasing applied field. However, a slight enhancement of the reflection loss with increasing applied field was observed for the frequency range of 3.0–10 GHz. Therefore, for our sample, the applied field for magnetic refrigeration does not reduce the reflection loss seriously in the frequency range of 3.0–15.0 GHz.

In conclusion, we have demonstrated that $LaFe_{11.6}Si_{1.4}C_{0.2}H_{1.7}$ has both excellent microwave absorption and giant magnetic entropy change around ambient temperature. The excellent electromagnetic wave absorption results from the large magnetic loss and dielectric loss as well as the efficient complementarity between relative permittivity and permeability. The giant MCE effect in this material provides an ideal technique for cooling the MAMs to avoid temperature increase and infrared radiation during microwave absorption. A prototype of magnetic cooling MAMs during microwave absorption is illustrated in Figure 1(c). To our knowledge, the results of giant microwave absorption of $-42$ dB and magnetic entropy change of $-20$ $Jkg^{-1}K^{-1}$ in one multifunctional material have never been reported. Our finding suggests that we can integrate the microwave

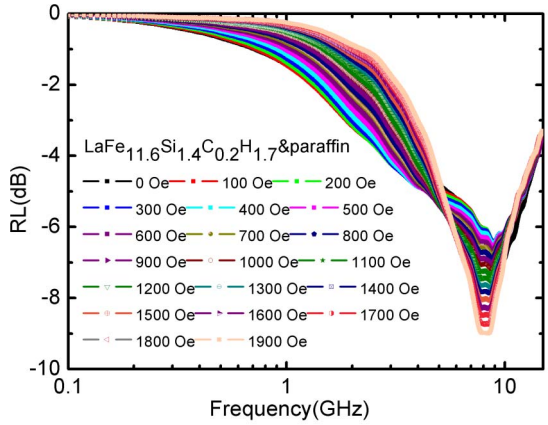


**Figure 8 | Field-dependence of reflection loss *RL* of for the $LaFe_{11.6}Si_{1.4}C_{0.2}H_{1.7}$/paraffin wax samples with thickness of 2.0 mm.**

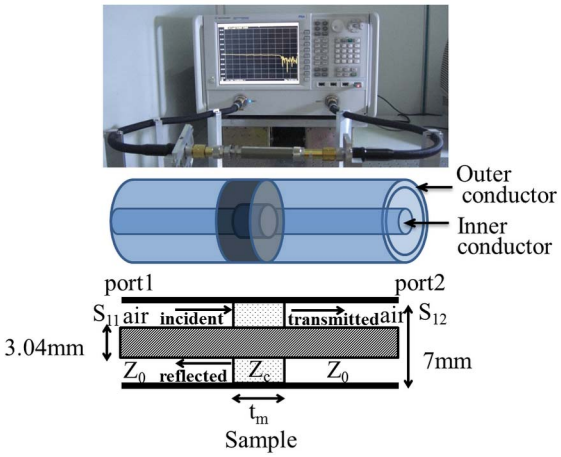


**Figure 9 | The measurement scheme of magnetic and dielectric spectra.** Coaxial line and sample.

absorption with magnetic refrigeration in one multifunctional material. This integration not only advances our understanding of the correlation between microwave loss and MCE, but also can open a new avenue to exploit microwave devices and electromagnetic stealth.

## Methods

The $LaFe_{11.6}Si_{1.4}C_{0.2}$ samples were prepared by arc-melting by appropriate proportions of Fe–C alloy, La, Fe, and Si with the purity better than 99.9 wt.%. The heat treatment was carried out in a quartz tube of high vacuum at 1373 K for 7 days. The bulk $LaFe_{11.6}Si_{1.4}C_{0.2}$ sample was crushed into small particles (<1.5 mm), and then hydrogenated at 523 K in a hydrogen atmosphere of ~0.6 MPa for a long time until saturation. Then, extraction of hydrogen to some extent from the saturated hydride was performed under a vacuum better than $5 \times 10^{-4}$ Pa at 250°C for different lengths of time. The hydrogen content was calculated from the variation of the sample weight before/after hydrogen absorption (desorption) and the weight was measured by an electronic analytical balance (AND GR-202) with a readability of 0.01 mg and a repeatability of 0.02 mg in the range 0–42 g. The weight of absorbed hydrogen was about 0.21 wt.% by weighing the mass before and after hydrogenation, and then the hydrogen content x was estimated to be 1.7. The method of hot extraction was generally used to determine the hydrogen content[28,29]. Powder x-ray diffraction data were obtained using Cu *Ka* radiation at room temperature. The lattice expansion as compared to the $LaFe_{11.6}Si_{1.4}C_{0.2}$ compound is $\Delta a/a = 1.1\%$, which is corresponding to $x \approx 1.7$ as previous report[28]. The hydrogen content obtained by weighing the mass before and after hydrogenation is consistent with the result estimated from lattice expansion. All magnetic measurements were performed on a commercial MPMS-7 type superconducting quantum interference device magnetometer.

The measurement scheme of magnetic and dielectric spectra is shown in Figure 9. For magnetic and dielectric spectra measurements, the $LaFe_{11.6}Si_{1.4}C_{0.2}H_{1.7}$ was ground to powders with grain size of 30–50 $\mu m$, then mixed homogenously with paraffin wax at the mass ratio of 4 : 1. The $LaFe_{11.6}Si_{1.4}C_{0.2}H_{1.7}$/paraffin wax samples were finaly pressed into the toroidal-shaped samples of 7.00 mm outer diameter and 3.04 mm inner diameter with the thickness from 2.0 to 8.3 mm. The scattering parameters of the toroidal samples that correspond to the reflection ($S_{11}$ and $S_{22}$) and transmission ($S_{21}$ and $S_{12}$) were measured by a vector network analyzer (Agilent N5224A) using a coaxial transmission–reflection method in the frequency range of 0.1–15.0 GHz. The toroids tightly fit into the coaxial measurement cell. Full two-port calibration was initially performed on the test setup in order to remove errors due to the directivity, source match, load match, isolation and frequency response in both the forward and reverse measurements. The complex permeability ($\mu_r$) and permittivity ($\varepsilon_r$) were determined from the scattering parameters using the Nicolson models[30].


1. Vinoy, K. J. & Jha, R. M. *Radar Absorbing Materials*, Kluwer Academic Publishers, Boston, MA (1996).
2. Shin, D. *et al.* Broadband electromagnetic cloaking with smart metamaterials. *Nature Commun.* **3**, 1213 (2012).
3. Che, R. *et al.* Microwave absorption enhancement and complex permittivity and permeability of Fe encapsulated within Carbon nanotubes. *Adv. Mater.* **16**, 40 (2004).
4. Li, B. W. *et al.* Enhanced microwave absorption in nickel/hexagonal-ferrite/polymer composites. *Appl. Phys. Lett.* **89**, 132504 (2006).
5. Liu, J. R. *et al.* Magnetic and electromagnetic wave absorption properties of α-Fe/Z-type Ba-ferrite nanocomposites. *Appl. Phys. Lett.* **88**, 062503 (2006).
6. Lagarkov, A. N. *et al.* High-frequency behavior of magnetic composites. *J. Magn. Magn. Mater.* **321**, 2082 (2009).
7. Srivastava, R. K. *et al.* Ni filled flexible multi-walled carbon nanotube–polystyrene composite films as efficient microwave absorbers. *Appl. Phys. Lett.* **99**, 113116 (2011).
8. Liu, L. *et al.* Microwave Loss in the High-Performance Dielectric $Ba(Zn_{1/3}Ta_{2/3})O_3$ at 4.2 K. *Phys. Rev. Lett.* **109**, 257601 (2012).
9. Pecharsky, V. K. & Gschneidner Jr., K. A. Giant magnetocaloric effect in $Gd_5Si_2Ge_2$. *Phys. Rev. Lett.* **78**, 4494 (1997).
10. Provenzano, V., Shapiro, A. J. & Shull, R. D. Reduction of hysteresis losses in the magnetic refrigerant $Gd_5Ge_2Si_2$ by the addition of iron. *Nature* (London) **429**, 853 (2004).
11. Tegus, O., Bruck, E., Buschow, K. H. J. & de Boer, F. R. Transition-metal-based magnetic refrigerants for room temperature applications. *Nature* **415**, 150–152 (2002).
12. Liu, J. *et al.* Giant magnetocaloric effect driven by structural transitions. *Nature Mater.* **11**, 620 (2012).
13. Moya, X. *et al.* Giant and reversible extrinsic magnetocaloric effects in $La_{0.7}Ca_{0.3}MnO_3$ films due to strain. *Nature Mater.* **12**, 52 (2013).
14. Hu, F. X. *et al.* Influence of negative lattice expansion and metamagnetic transition on magnetic entropy change in the compound $LaFe_{11.4}Si_{1.6}$. *Appl. Phys. Lett.* **78**, 3675–3677 (2001).
15. Shen, B. G. *et al.* Recent progress in exploring magnetocaloric materials. *Adv. Mater.* **21**, 4545–4564 (2009).
16. Snoek, J. L. Gyromagnetic resonance in ferrites. *Nature* **160**, 90 (1947).
17. Wang, F. W. *et al.* Strong interplay between structure and magnetism in the giant magnetocaloric intermetallic compound $LaFe_{11.4}Si_{1.6}$: a neutron diffraction study. *J. Phys.: Condens. Matter* **15**, 5269 (2003).
18. Mu, G. *et al.* Microwave absorption properties of hollow microsphere/titania/M-type Ba ferrite nanocomposites. *Appl. Phys. Lett.* **91**, 043110 (2007).
19. Harris, V. G. Modern Microwave Ferrites. *IEEE Trans on Magn.* **48**, 1075 (2012).
20. Wu, M. Z. *et al.* Microwave magnetic properties of $Co_{50}/(SiO_2)_{50}$ nanoparticles. *Appl. Phys. Lett.* **80**, 4404 (2002).
21. Watts, P. C. P., Hsu, W. K., Barnes, A. & Chambers, B. High permittivity from defective multiwalled carbon nanotubes in the X-Band. *Adv. Mater.* **15**, 600 (2003).
22. Ramo, S., Whinnery, J. R. & Duzer, T. V. *Fields and Waves in Communication Electronics* Wiley, New York 1984.
23. Naito, Y. & Suetake, K. Application of ferrite to electromagnetic wave absorber and its characteristics. *IEEE Trans. Microwave Theory Tech.* **19**, 65 (1971).
24. Davalos, A. L. & Zanette, A. Fundamentals of Electromagnetism. Springer Verlag, Berlin 1999.
25. Wadhawan, A., Garrett, D. & Perez, J. M. Nanoparticle-assisted microwave absorption by single-wall carbon nanotubes. *Appl. Phys. Lett.* **83**, 2683 (2003).
26. Zimm, C. *et al.* Design and performance of a permanent-magnet rotary refrigerator. *Inter. J. Refrigeration* **29**, 1302 (2006).
27. Fujita, A., Fujieda, S., Hasegawa, Y. & Fukamichi, K. Itinerant-electron metamagnetic transition and large magnetocaloric effects in $La(Fe_xSi_{1-x})_{13}$ compounds and their hydrides. *Phys. Rev. B.* **67**, 104416 (2003).
28. Lyunina, J. *et al.* Multiple Metamagnetic Transitions in the Magnetic Refrigerant $La(Fe,Si)_{13}H_x$ *Phys. Rev. Lett.* **101**, 77203 (2008).
29. Chen, Y. F. *et al.* Magnetic properties and magnetic entropy change of $LaFe_{11.5}Si_{1.5}H_y$ interstitial compounds. *J. Phys.: Condens. Matter.* **15**, L161 (2003).
30. Nicolson, A. M. & Ross, G. F. Measurement of intrinsic properties of materials by time-domain techniques. *IEEE Transactions on Instrumentation and Measurement.* **IM19**, 377–382 (1970).


## Acknowledgments

This work was supported by the National Basic Research Program of China (973 program, Grant Nos. 2012CB933102, 2011CB921801 and 2010CB93420) and the National Natural Sciences Foundation of China (11174351, 11274357, 11034004, and 51021061).

## Author contributions

Z.H.C. planned the experiments. N.N.S. and Y.J.K. carried out the microwave and magnetic entropy changes experiments. H.Z. prepared the sample. H.T.Y. and X.Q.Z. setup the microwave measurements. B.G.S. explained the magnetocaloric effect. All the co-authors contributed to the analysis and discussion for the results. Z.H.C. wrote the paper with the input from all the co-authors.

## Additional information

**Competing financial interests:** The authors declare no competing financial interests.

**How to cite this article:** Song, N. *et al.* Integrating giant microwave absorption with magnetic refrigeration in one multifunctional intermetallic compound of $LaFe_{11.6}Si_{1.4}C_{0.2}H_{1.7}$. *Sci. Rep.* **3**, 2291; DOI:10.1038/srep02291 (2013).